Thermo-optic waveguide digital optical switch using symmetrically coupled gratings

De-Gui Sun[1, 2], Zhiying Liu[2], Ying Zha[1], Wenyuan Deng[1], Ying Zhang[1], and Xiaoqi Li[1]

1) State Key Laboratory of Applied Optics, Changchun Institute of Optics, Fine Mechanics and Physics, Chinese Academy of Sciences, 16 East Nanhu Street, Changchun, JL 130031, China
2) School of Optoelectronic Engineering, Changchun University of Science and Technology 7089 Weixing Road, Changchun, JL 130022, China
deguisun_b@yahoo.com

Abstract: A 2x2 digital optical switch using two symmetrical unidirectional Bragg grating couplers is proposed and studied in this paper. A low-loss polymer is used as waveguide material, and the Bragg grating coupling efficiency is optimized to be 22%, then the unidirectional coupling efficiency of 99.9% is achieved in theory. The performance of the switch based on the unidirectional couplers with Bragg gratings is theoretically modeled and simulated. Finally, the 2.4dB insertion loss, the -17dB crosstalk between two output ports, the 28 dB extinction ratio, the 1.5ms response speed and the 87mW power consumption are experimentally demonstrated with this regime.

OCIS codes: (130.3120) Integrated optics devices; (060.1810) Couplers, switches, and multiplexers

References and Links

1. R. Ramaswami and K. N. Sivarajan, "Wavelengh routing network," in Optical Networks: A Practical Perspective, J. Mann, Y. Overton, C. Palmer and K. Johnson, eds. (Acadamic, San Francisco, Calif., 1998), pp. 329-389.
2. G. I. Papadimitriou, C. Papazoglou, and A. S. Pomportis, "Optical switching: switch fabrics, techniques, and architectures," J. Lightwave Technol. **21,** 384-405 (2003).
3. T. Yoshimura, S. Tsukada, S. Kawakami, M. Ninomiya, Y. Arai, H. Kurokawa, and K. Asama, "Three-dimensional micro-optical switching system architecture using slab-waveguide-based micro-optical switches," Opt. Eng. **42,** 439-446 (2003).
4. R. Kasahara, M. Yanagisawa, T. Goh, A. Sugita, A. Himeno, M. Yasu, and S. Matsui, "New structure of Silica-based planar lightwave circuits for low-power thermooptic switch and its application to 8x8 optical matrix switch," J. Lightwave Technol. **20,** 993-1000 (2000).
5. M. C. Oh, H. J. Lee, M. H. Lee, J. H. Ahn, and S. G. Han, "Asymmetric X-junction thermooptic switches based on fluorinated polymer waveguides," IEEE Photon. Technol. Lett. **10,** 813-815 (1998).
6. N. Keil, H. H. Yao, and C. Zawadzki, "(2x2) digital optical switch realized by low cost polymer waveguide technology," Electron. Lett. **32,** 1470-1471 (1996).
7. S. S. Lee, and S. Y. Shin, "Polymeric digital optical switch with a linear branch and an optimized coupling region," in Integrated Optics Devices: Potential for Commercialization, S. I. Najafi, M. N. Armenise, eds., Proc. SPIE **2997,** 126-134 (1997).
8. D. G. Sun and Ray T. Chen, "Polymer-based highly multimode electro-optic waveguide modulator," Appl. Phys. Lett. **72**, 3139-3141 (1998).
9. P. Pascal et al., "Optimized coupling of a Gaussian beam into a waveguide with a grating coupler: comparison of experimental and theoretical results," Appl. Opt. **36,** 2443-2447 (1997).
10. D. G. Sun, C. Zhao, and Ray T. Chen, "Intraplane to interplane optical interconnects with high diffraction efficiency electrooptic grating," Appl. Opt. **36,** 629-634 (1997).
11. A. Yariv and P. Yeh, Optical Wave in Crystals, Wiley, (New York 1994).
12. Y. Hida, H. Onose, and S. Imamura, "Polymer waveguide thermooptic switch with low electric power consumption at 1.3 μm," IEEE Photon. Technol. Lett. **5**, 782-784 (1993).
13. M. B. J. Diemeer, J. J. Brons, and E. S. Trommel, "Polymeric optical waveguide switch using the thermooptic effect," J. Lightwave Technol. **7,** 449-453 (1989).
14. BCB 3022-25,from Dow Chemical Co., Midland, MI 48674, http://www.dow.com/cyclotene/prod/402235.htm.

#7632 - $15.00 USD Received 1 June 2005; revised 28 June 2005; accepted 29 June 2005

1. Introduction

The space-division optical switch is always a key device for realizing intelligent optical communication systems and has been playing a significant role in the development of industrial optical networks. [1,2] In the past decade, various architectures of optical switches are investigated and developed to possess different characteristics with respect to different environments of applications. In particular, the waveguide thermooptic switches receive much more research and much accomplishment has been made. [3,4] The thermooptic waveguide devices based on polymers and other temperature sensitive materials have shown an exciting essence in the low-speed operations because of their great flexibility in fabrication and processing. [4-6] The thermooptic waveguide devices can be built with glass, silica, crystal and polymer because only upper modulating electrodes are needed. Thereby the polymer-based thermooptic waveguide devices have been successively applied into fiber-optic communications systems and have been receiving more and more attention in this field.

Basically, the waveguide thermooptic optical switches mainly involve two mechanisms, one is based on the Mach-Zehnder interferometer (MZI) structure as a 1x2 or 2x2 switching unit, and the other is based on a digital thermooptic effect to perform 1x2 or 2x2 switching operations, which is referred to as digital optical switch (DOS). The polymer-based DOS represents its merit in extinction ratio, device structure and size, but in some proposed DOS's, the structures of heaters for thermooptic waveguide DOS's are relatively more complicated, resulting in relatively higher power consumption and higher optical loss. [5-7]

In this paper, a new DOS architecture based on polymer waveguides and the symmetric couplers of two Bragg gratings is demonstrated. The theoretically predicted data basically agree with the experimentally measured results.

2. Design of devices

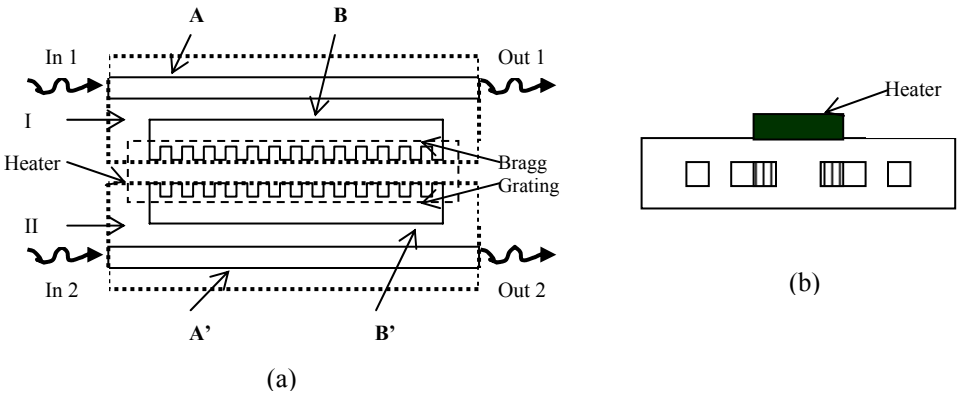

Fig. 1. Configuration of a 2x2 themo-optic waveguide switch using unidirectional couplers with Bragg gratings, where Fig. 1(a) is the top view and Fig. 1(b) is the cross-section

The new waveguide digital optical switches (DOS's) studied in this work is composed of two symmetrically placed unidirectional couplers with Bragg gratings and a heater covering the Bragg grating area. This DOS is schematically depicted in Fig. 1, where Fig. 1(a) is the top view of the device configuration and Fig. 1(b) the cross-section. A heater is deployed to exactly cover the two Bragg gratings. The two unidirectional couplers are labeled as Coupler I and Coupler II, respectively. Unidirectional coupler I contains one long straight waveguide channel **A** for guiding light waves and one short waveguide channel **B** having a Bragg grating at the outside edge for coupling light waves, and unidirectional coupler II contains one long straight waveguide channel **A'** for guiding light waves and one short waveguide channel **B'**

#7632 - $15.00 USD Received 1 June 2005; revised 28 June 2005; accepted 29 June 2005

having a Bragg grating at the outside edge for coupling light waves. So, the channels **A** and **A'** are referred to as guiding channels and the channels **B** and **B'** are referred to as coupling channels. We only take unidirectional coupler I to analyze the operating principle for a light wave. If channel **B** had no Bragg grating, waveguide channels **A** and **B** form a regular waveguide coupler and a light wave can be bi-directionally coupled between these two channels. But, now because a Bragg grating is deployed for channel **B**, when a light wave is coupled from **A** to **B**, it cannot be coupled back to **A**, instead it is coupled out by the Bragg grating. In the inverse manner, when a light wave strikes on the Bragg grating, it can be coupled into waveguide channel **B**, and then can be gradually coupled into channel **A**. Thus, this sub-system is a unidirectional coupler. In the same manner, the sub-system labeled as II has the same structure as the sub-system labeled as I, so it is also a unidirectional coupler. These two unidirectional couplers symmetrically placed as shown in Fig. 1 can form a special waveguide system that has a 2x2 switching function. Namely a thermooptic 2x2 DOS is formed. The unidirectional coupling process with Bragg grating can not only help this system perform a 2x2 DOS, but also improve optical energy transfer efficiency, resulting in a much lower crosstalk between two output ports in switching operations. This DOS is similar to an X-junction-based switch, but the architecture of this 2x2 DOS is much simpler than that of the X-junction based DOS's. [6,7] In fact, the effect of grating-assistant waveguide coupling has been studied and demonstrated by some researchers. [8-10]

3. Theoretical discussion

For the goal of achieving a high on-off extinction ratio with Bragg gratings in the DOS architecture, the primary concern is the coupling efficiency η_g of grating, which directly impacts the unidirectional coupling efficiency η_u of the unidirectional couplers. If no electric power is applied onto the heater, the Bragg grating-coupler exists, so the coupling from channel **A** to channel **B** is not limited, but its inverse process is limited. In contrast, if an electric power is applied onto the heater, an negative index modulation ($\Delta n_m < 0$) is induced, then the coupling grating does not exist, either the coupling process from channel **A** to channel **B** or its inverse process is not limited, i.e. a bi-directional coupling process. The coupling efficiencies of both the unidirectional and the bi-directional coupling processes are expressed by Eqs. (1) and (2), respectively, as [8]

$$\eta_u = \sum_{n=0}^{m} \frac{k_c^2}{\psi^2} \eta_g \sin^2[\psi(m+1)\Delta L][1-\frac{k_c^2}{\psi^2}\eta_g \sin^2(\psi m \Delta L)] \tag{1}$$

$$\eta_b = \frac{k_c^2}{\psi^2}\sin^2(\psi L) \tag{2}$$

where η_g is the coupling efficiency of the Bragg grating, which is determined by the structure of the Bragg grating, k_c is the coupling constant between two waveguide channels, L is the interaction length, ΔL is a selected length within which the coupled-out optical energy from the guiding channel **A** to the coupling channel **B** is uniform, m is the integer closest to $L/\Delta L$, ψ is defined by $\psi = (k_c^2 + \Delta^2)^{1/2}$ with $\Delta = k|N_a - N_b|/2$ where $k = 2\pi/\lambda$ is the wave number, N_a and N_b are the effective refractive indices of the guided modes in channels **A** and **B**, respectively.

As mentioned above, the alternating change of the unidirectional coupling and the bi-directional coupling in the 2x2 DOS studied in this work is completely determined by the difference of the coupling efficiencies between the unmodulated state (i.e., $\Delta n_m = 0$) and the

#7632 - $15.00 USD Received 1 June 2005; revised 28 June 2005; accepted 29 June 2005

modulated state (i.e., $\Delta n_m \neq 0$). For the polymer-based thermo-optic switch, the modulated amount of refractive index is $\Delta n_m = -(dn/dT)\Delta T$, where dn/dT is the corresponding thermooptic coefficient and ΔT is the change of temperature. Note from (1) and (2) that the unidirectional coupling efficiency can be up to 100% in theory by appropriately choosing ψ, η_g and L, and the bi-directional coupling efficiency can be zero in theory by appropriately choosing the values of ψ and L. Therefore, the coupling efficiency difference between the unmodulated state and the modulated state can be achieved to a high value with the waveguide-Bragg-grating based 2x2 DOS regime, resulting in a much higher extinction ratio at each of output ports and a much lower crosstalk between two output ports.

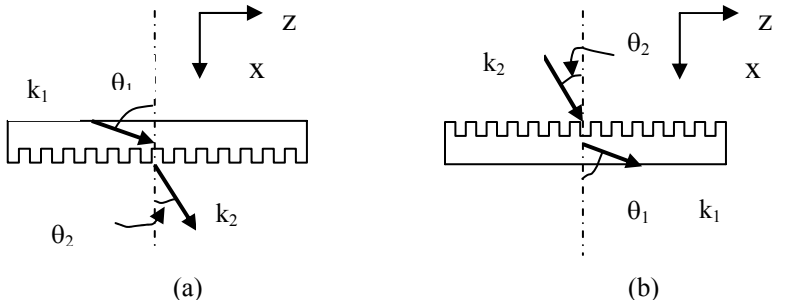

Fig. 2. Schematically coupled processes of optical beams in the waveguide-Bragg-grating regime: (a) the coupled-out case of an optical beam from waveguide channel; (b) the coupled-in case of an optical beam from outside

In order to investigate the coupling process of the unidirectional coupler, we illustrate the schematics of both the coupling-out and coupling-in Bragg gratings as depicted in Fig. 2(a) and Fig. 2(b), respectively, where k_1 and k_2 are the wave numbers of the incident and coupled optical beams, respectively. For the coupling-out and coupling-in cases shown in Fig. 2(a) and Fig. 2(b), respectively, we have Eqs. (3a) and (3b), respectively, as [10,11]

$$\beta_{1,2} = \frac{2\pi}{\lambda} n_{1,2} \sin\theta_{1,2}, \tag{3a}$$

$$\alpha_{1,2} = \frac{2\pi}{\lambda} n_{1,2} \cos\theta_{1,2} \tag{3b}$$

where $n_1 = n_{co}$ and $n_2 = n_{cl}$ are the refractive indices of waveguide core and cladding layer, respectively, λ is the wavelength, and θ_1 and θ_2 are the incident angle and the coupled angle of optical beam, respectively. Note from Fig. 2 that the coupling case that we are discussing here is a co-directional coupling, thus we define the coupling efficiency of the waveguide Bragg grating system η_g as [10,11]

$$\eta_g = \left[\frac{\sin(D_g \cdot \Delta\alpha)}{D_g \cdot \Delta\alpha}\right]^2 \sin^2(K_g \cdot D_g) \tag{4a}$$

$$K_g = \frac{\omega^2 \mu}{2\sqrt{\alpha_1 \alpha_2}} \vec{P}_1 \cdot \Delta\varepsilon \vec{P}_2 \tag{4b}$$

#7632 - $15.00 USD Received 1 June 2005; revised 28 June 2005; accepted 29 June 2005

where $\Delta\alpha = |\alpha_1 - \alpha_2|$ indicates the mismatch of the light wave momentum of the grating coupling system at x direction, K_g is the coupling constant of Bragg grating, D_g is the depth of the Bragg grating , ω is the angular frequency of the light wave, $\vec{P}_1$ and $\vec{P}_2$ are unit wave vectors of beams k_1 and k_2, μ is the permeability of waveguide material, and $\Delta\varepsilon$ is the increment of dielectric constant ε of waveguide material. Taking a look at the unidirectional coupler I shown in Fig. 1 yields that the unidirectional coupler contains two coupling processes, one is the regular bi-directional coupling between two waveguide channels **A** and **B**, and the other one is the coupling-out or coupling-in of the Bragg grating. Thereby, with (1) through (4), we can simulate the performance of the unidirectional coupler.

In the thermooptic modulation based devices, the thermal conduction is the principal mechanism. If P and Δn respectively stand for the power consumption and the required index modulation, the relation between P and Δn can be defined by [12,13]

$$P = \kappa_W \frac{W_H L_H}{t_W}(1 + 0.88\frac{t_W}{W_H}) \cdot \Delta T \tag{5}$$

where $\Delta T = \Delta n / (dn / dT)$, κ_W is the thermal conductivity of the heated waveguide material, W_H and L_H are the width and the length of heater, respectively, and t_W is the thickness of the waveguide system, i.e., the required distance of heat flow. In the MZI based thermooptic switches, the index modulation Δn is required to produce an optical phase change of $\lambda/2$, i.e., $\Delta n L_H = \lambda/2$. But, for the DOS studied in this work, the index modulation Δn is for eliminating the phase grating, i.e., the refractive index difference between the core layer and the cladding layer. Note from (5) that Δn, $W_H \cdot L_H$ and t_W are the selectable parameters in the DOS system, and a small Δn, a small $W_H \cdot L_H$ and a large t_W are desired in order to lower the power consumption P of implementing switching operations. Polymers have much higher thermooptic coefficient ($dn/dT \sim -1\times10^{-4} K^{-1}$), [5,13] and relatively smaller thermal conductivity ($\kappa_W = 0.17 / m \cdot K$), [13] so they are suited to the DOS's according to (5) and have been deployed for investigating various architectures of DOS's. [5-7]

4. Performance simulations and optimization

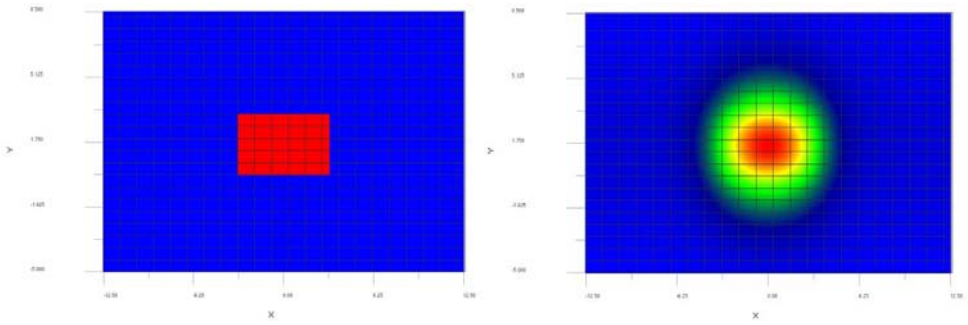

(a) (b)

Fig. 3. BPM simulation results of single-mode waveguide structure: (a) the cross-section of waveguide channel; (b) the beam profile of a single-mode

#7632 - $15.00 USD Received 1 June 2005; revised 28 June 2005; accepted 29 June 2005

For the DOS regime investigated in this work, the single-mode operations are required. For the goal of the performance simulation of the 2x2 DOS system, we select the commercially available high transparency polymer polybisbenzocyclobutane (BCB) for waveguide materials because this polymer has a set of core and cladding types with the refractive indices of 1.552 and 1.544, respectively, and the relatively lower propagation loss of about 0.5dB/cm at λ=1550nm wavelength. [14] With BPM software simulator, we obtain the waveguide size of 8.0μmx4.0μm for single mode-mode operations as shown in Fig. 3, where Fig. 3(a) is the cross-section of the waveguide structure and Fig. 3(b) is the image of a single-mode beam profile for the TE input light waves at λ=1550nm. In this system, the thickness of both the upper and the lower cladding layers is selected as 8.0 μm.

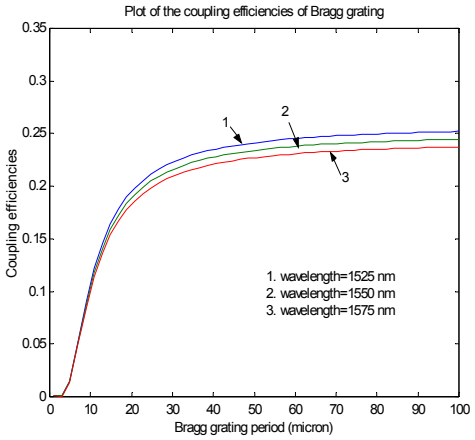

Fig. 4. Simulation for the coupling efficiencies of Bragg grating vs. Bragg period with respect to three typical wavelength values

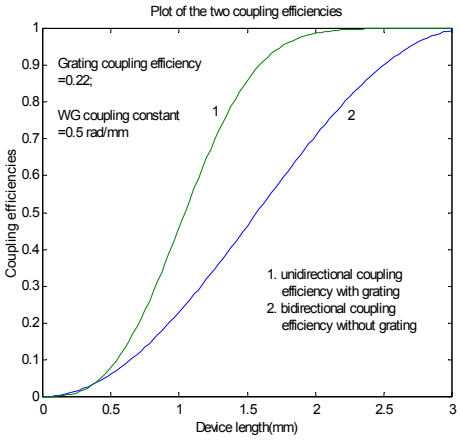

Fig. 5. Simulation for both the coupling efficiencies unidirectional process and the normal bi-directional coupling process

When the waveguide size for both **A** and **B** is taken as 8.0 μm wide and 4.0 μm thick, the diffraction angle in the waveguide for the fundamental mode is $\theta_1 \approx 85^\circ$ at λ=1550nm wavelength. By designing the grating depth as 2.0 μm and with (3) and (4), we simulate the most important parameter of the waveguide-Bragg-grating regime, the coupling efficiency η_g of Bragg grating with respect to the three typical wavelength values of 1525nm, 1550nm and 1575nm and obtain the results as shown in Fig. 4. Note that, as expected, the final coupling efficiency of Bragg grating is almost kept at a constant of 0.22 when Λ is increased to more than 20 μm, but the coupling efficiency η_g of Bragg grating is dependent on the wavelength in the period range from 20 μm to 100 μm though the dispersion of waveguide material is ignored. (1) and (2) are for respectively calculating the unidirectional coupling efficiency of the waveguide-Bragg-grating system and the bi-directional coupling between two single-mode waveguide channels in the system shown in Fig. 1. η_g and k_c are two important factors in the DOS and play significant roles in speeding up both the uni- and bi-directional coupling processes, resulting in shortening the device length and improving the on-off extinction ratio of system, and determined by the Bragg grating structure and the waveguide coupler architecture, respectively. Further, when the **A** and **B** are designed to have the same size, we have $\Delta = 0$ and $\psi = k_c$, resulting in the highest values of the efficiency of the bi-directional coupling process.

#7632 - $15.00 USD Received 1 June 2005; revised 28 June 2005; accepted 29 June 2005

By designing a waveguide size of 8x4μm^2 and a spacing of 3μm between two waveguide channels, a coupling length of 3mm and a k_c value of $0.5 rad/mm$ are obtained with BPM software simulator. Thus, with (1) and (2), we simulate the uni- and bi-directional coupling processes as functions of the grating length and obtain the results as shown in Fig. 5, where curves 1 and 2 are the uni- and bi-directional coupling processes, respectively. Note that the maximal value of the bi-directional coupling curve occurs at the coupling length of 3 mm, but the unidirectional coupling curve has almost approached to 100% value at the coupling length of 2.4 mm. The results in Fig. 5 are very conducive for both calculating the Bragg grating length and designing the minimum length of waveguide coupling channels, which are required to have the double lengths of the uni- and bi-directional couplings. Thus, the Bragg grating is required to be more than 4.8 mm and the coupling waveguide channels **B** and **B'** are exactly required to be 6 mm.

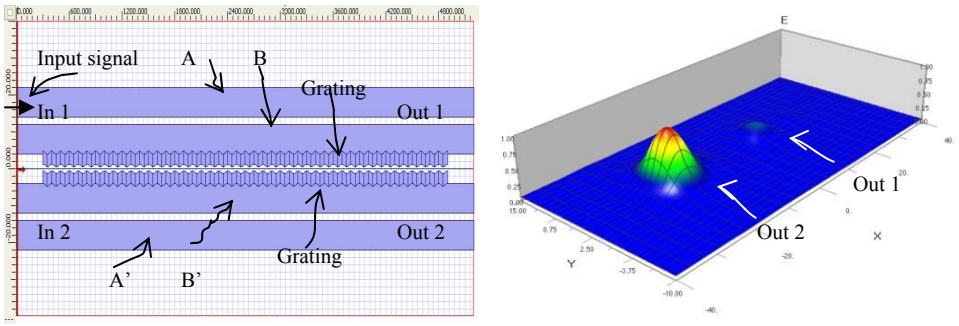

(a) (b)

Fig. 6. BPM simulation results of the DOS when a light signal is input from In 1: (a) the top view of DOS system before the electric power is applied; (b) the beam profile of output signal

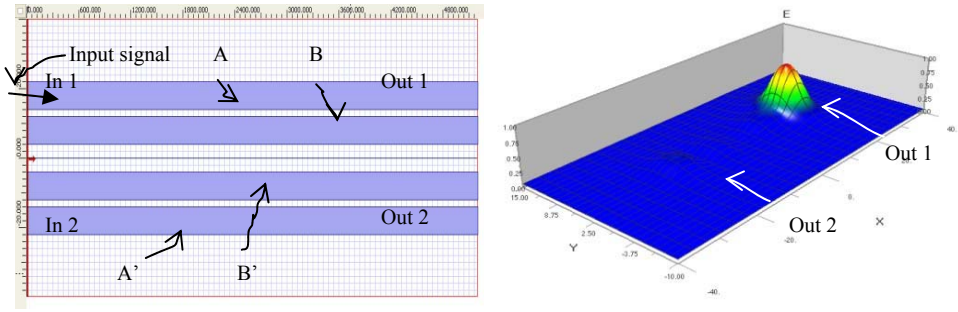

(a) (b)

Fig. 7. BPM simulation results of the DOS when a light signal is input from In 1: (a) the top view of DOS system after the Bragg gratings are eliminated by an electric power; (b) the beam profile of output signal

With simulation values of waveguide parameters obtained above and BPM software simulator, an optimal structure of the DOS using two symmetric unidirectional couplers assisted by Bragg gratings is obtained. The separate between the guiding channel **A** and coupling channel **B** is 3.0 μm, the separate between two coupling channels **B** and **B'** is 8 μm, the length of all waveguide channels **A**, **B**, **A'** and **B'** is 5.2 mm, the length and the period of the Bragg gratings are 4.9 mm and 50 μm, respectively. Before a modulation power is applied onto the heater, the schematic of the 2x2 DOS with Bragg gratings and the output beam profile at the unmodulated state for an input optical signal are depicted in Fig. 6(a) and Fig. 6(b), respectively. After a modulation power is applied onto the heater, the schematic of the

#7632 - $15.00 USD Received 1 June 2005; revised 28 June 2005; accepted 29 June 2005

2x2 DOS without Bragg gratings and the output beam profile at the modulated state for the optical signal are depicted in Fig. 7(a) and Fig. 7(b), respectively. In accordance with Fig. 6(b) and Fig. 7(b), the -16dB and -24dB crosstalk values between two output ports are obtained and the 0.3dB and 0.8dB optical losses at the die level are calculated. In our simulation, the main sources of optical loss including propagation loss from waveguide channels and materials, the excess losses from the waveguide and the Bragg grating couplings are considered. It can be concluded that the simulation results from BPM simulator are very closed to the calculation values from (1) and (2). Further, by taking $W_H = 8.0\mu m$, $L_H = 5.0mm$ and waveguide thickness $t_W = 16\mu m$, we obtain the approximate power consumption of 82mW with (5).

The cladding polymer material used in this work is produced with mixing the other material sol-gel to the polymer BCB, then the cladding film is spin-coated and a long-term UV curing is processed. As a consequence, its refractive index is approximately decreased from 1.552 to 1.544 and its thermooptic constant is approximately decreased from $-1.15\times10^{-4}K^{-1}$ to $-0.2\times10^{-4}K^{-1}$. When an approximate 80mW electric power is applied onto the heater, changes of refractive indices in core and cladding are -0.008 and -0.0014, respectively. Then, we have $n_{co}^{'} = 1.544$ and $n_{cl}^{'} = 1.5426$, further$\Delta n'=1.4\times10^{-3}$., i.e., the phase difference of the modulated Bragg gratings. Such a weak phase difference is not sufficient to have the coupling function of grating, namely, the Bragg gratings disappear.

5. Experiments

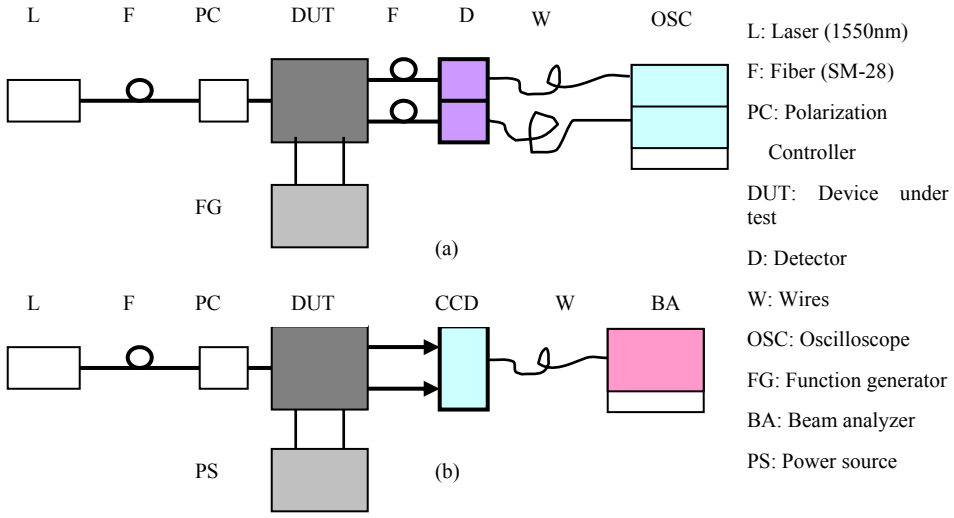

Fig. 8. Experimental setup for measuring the performance of the 2x2 DOS during the switch is being modulated by a rectangular alternating electric signal: (a) for detecting the modulated output signals at output ports in switching process; (b) for detecting the beam profile of two optical outputs

In the mask design for fabricating waveguides with photolithographic technique, the Bragg gratings are arranged on the edges of coupling channels according to the calculated data. Because the Bragg gratings are formed along the horizontal direction of the device plane, their diffractions are exactly suitable for the switching processes of optical signals between the two output ports. Two experimental setups are built as shown in Fig. 8(a) and Fig. 8(b) for respectively measuring the switching process of the DOS during it is being modulated by a alternating electric signal and displaying beam profiles of the output signals of the DOS.

#7632 - $15.00 USD Received 1 June 2005; revised 28 June 2005; accepted 29 June 2005

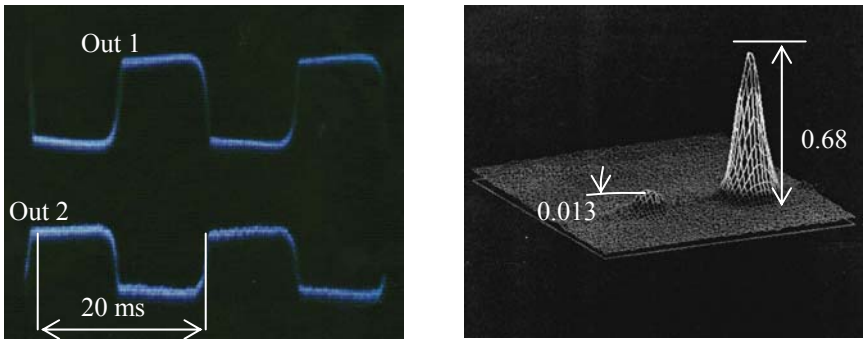

(a) (b)

Fig. 9. Experimental results of switching process during the switch is being modulated by a alternating electric signal: (a) the picture of the modulated output signals at output ports taken on the oscilloscope in switching process; (b) the beam profiles of two optical outputs

Figure 9 shows the experimental results of switching process with the fabricated devices, where Fig. 9(a) is the picture of the modulated output signals at two output ports taken on oscilloscope during the switch is being modulated by a rectangular alternating electric signal and Fig. 9(b) is the beam profiles of the two outputs when a drive power of 87mW is applied onto the device. An on-off extinction ratio of 28 dB, a crosstalk of -17 dB between two outputs are measured, the insertion loss of 2.4 dB are obtained. The response speed of the DOS is that the rise time and the fall time are approximately 1.5 ms and 1.3 ms, respectively. The main sources of coursing optical insertion loss should be from the propagation loss, the scattering of the waveguides and the Bragg grating. Here the reason for that the extinction ratio value measured in experiments is less than the simulation result implies that the thermooptic modulation is more possible to insulate the optical signals between two coupling channels B and B'. The simulation result of optical loss on die level is 1.1 dB and the measured value of insertion loss is 2.4 dB, which implies the total fiber-waveguide coupling loss is approximately 1.3 dB. The reason for why the measured result of power consumption is higher than the calculated value is the tested device is only 12 μm thick instead of 16 μm.

6. Conclusion

A new waveguide DOS configuration composed of two symmetric unidirectional couplers with Bragg gratings is demonstrated in this paper. An insertion loss of 2.4 dB, an on-off extinction ratio of 28 dB and a crosstalk of -17 dB between two outputs are achieved in experiments. Because the principle for DOS switching operations differs from all other DOS structures, the index change for this regime is much less and a relatively lower power consumption of about 87mW is achieved for switching operations. In addition, the device size and complexity of this new 2x2 DOS are improved much compared with others, so it can be further improved to be a switching unit for constructing large-scale matrix switches. The experimental results basically agree with the theoretically calculated data. The attributes of this new DOS's observed in experiments make the new DOS regime have a large room for continuous research and promising applications.

Acknowledgments

This is supported by the 100-person-plan foundation of Chinese Academy of Sciences.

#7632 - $15.00 USD Received 1 June 2005; revised 28 June 2005; accepted 29 June 2005